Pergamon

Int. J. Heat Mass Transfer. Vol. 40, No. 14, pp. 3275–3282, 1997

Printed in Great Britain
0017–9310/97 $17.00+0.00

PII: S0017-9310(96)00389-4

Effect of positioning the axis of a lamellar rotor model of a sucking and forcing regenerative exchanger on the intensity of convective mass/heat transfer

B. BIENIASZ, K. KIEDRZYŃSKI, R. SMUSZ and J. WILK

Thermodynamics Department, Rzeszów University of Technology, ul. W. Pola 2, 35-959 Rzeszów, Poland

(*Received* 8 *August* 1996 *and in final form* 14 *November* 1996)

Abstract—Mean values of the convective mass/heat transfer coefficients for two porous structures—differing in both profile and the value of D_h—of the rotor of a heat regenerator were measured for horizontal and vertical positions of the axis. The flow in short curved ducts of the immovable model was forced by the pump. The results of electrolytic measurements were independent of the positioning of the axis. Final correlations of the j_M-factor or *Sh* vs *Re* are almost identical for both duct geometries for the common range of *Re*. An example of the use of the results for simple heat transfer calculations illustrates a problem. The results are valid for a constant-potential/temperature boundary condition. © 1997 Elsevier Science Ltd.

INTRODUCTION

The functioning, application possibilities, and main thermal features of the sucking and forcing regenerative heat exchanger invented by de Fries have been discussed, among others, by Bieniasz and Wilk [1]. They presented the results of electrolytical investigations of the mean value of the mass/heat transfer coefficient at the surface of two different, curved short ducts of the stationary porous rotor with a horizontal axis. Two types of rotor pattern resulted from the combination of corrugated and flat sheets of the pattern.

In the meantime, suggestions have appeared for the possible influence of the hydrostatic pressure of an electrolyte on its flow rate in particular ducts of the model, and thereby on the mean value of the mass transfer coefficient at the horizontal position of the axis of the model. The authors doubted the theoretical possibility of such a phenomenon in the entirely filled test section of the horizontal axis, as described in ref. [1]: nevertheless, they yielded to the temptation of carrying out conclusive experiments to solve the problem. In this connection, they decided to look at both horizontal and vertical axes.

The second reason for recommencing the experiments was the idea of filling the side half-ducts to rectify the type I model of the rotor in order to obtain a better consistency of the real and measured values of the mean hydraulic diameter of the duct. The above consistency could additionaly be heightened—for both types of rotor—by the application of an about 3–5 μm thin, almost ideally smooth Teflon layer instead of the previous about 200 μm Araldite layer to the surface.

EXPERIMENTAL METHOD

The experimental technique—an electrolytic one—and method, as well as the rig, were the same as in ref. [1], where they were thoroughly described. They enabled an experiment with a boundary condition of a constant potential for the nickel cathode of the model to be carried out. The test section, particularly the shapes and dimensions of all elements of the models, also remained unchanged. The only change, except using a Teflon layer to cover the non-working surfaces of the model elements, occurs in the type I model, and is depicted in Fig. 1. The main difference is that the volume between both side-sheets and the flanges of the test section was filled by Araldite to eliminate the flow of electrolyte through the side half-ducts. Arrows indicate the working surfaces of the cathodes. Those of the type II model were used both individually and simultaneously when supplied in a parallel fashion. The value of the working surface area of a single corrugated sheet of the model was equal to 49.9 cm^2, and that of a flat sheet was 41.9 cm^2. The only quantities measured during the course of the experiment—except for the volumetric flow rate—were the plateau current and the bulk concentration of ferricyanide ions in the electrolyte.

After installing the test sections and activating particular cathodes, about 7–10-day trials followed using the working electrolyte, at the end of which the repeatability of the measured results was checked for each cathode. The trials and measurements of the mean value of the mass transfer coefficient lasted for about 3 h a day. Then, three separate measurements—one a day—were made for a full range of *Re*, achievable on the rig, for each working surface or combination of

NOMENCLATURE

A_H	overall surface area of heat transfer for the rotor
a	thermal diffusivity
C_b	bulk concentration of ferricyanide ions
c_{pg}	specific heat capacity of the gas at p = constant
D	diffusivity of ferricyanide ions in the electrolyte
D_h	mean hydraulic diameter of the duct
F	Faraday constant
Gz_L	Graetz number, $\frac{\pi}{4}\frac{wD_h^2}{aL}$
h	mean heat transfer coefficient for the whole surface of the duct
h_D	mean mass transfer coefficient, $I_p/(AFC_b)$
I_p	plateau current
j_M	mean Chilton–Colburn coefficient for mass transfer, $St_M\, Sc^{2/3}$
L	length of the duct
Nu	mean Nusselt number for the whole surface of the duct, hD_h/λ_g
Re	mean Reynolds number based on D_h, wD_h/ν or w_gD_g/ν_g
Sc	Schmidt number, ν/D
Sh	mean Sherwood number, h_DD_h/D
St_H	mean heat transfer Stanton number, $h/(c_{pg}\rho_g w_g)$
St_M	mean mass transfer Stanton number, h_D/w
$\dot{V}_N$	air flux
w, w_g	mean velocity, in the mean cross-section area of the duct, of electrolyte and gas, respectively.

Greek symbols

λ_g	thermal conductivity of gas
ν, ν_g	kinematic viscosity of electrolyte and gas, respectively
ρ_g	mean density of gas in the mean cross-section of the duct.

surfaces—as in the case of the type II model—to obtain mean values of the mass/heat transfer coefficient. All this was done for both horizontal and vertical positions of the axis of the test section.

The temperature of the electrolyte was equal to 25°C, the concentration of ferricyanide ions in it was $50.0–85.5 \times 10^{-4}$ kmol m^{-3}, and the range for the volumetric flow rate was $0.11–0.92 \times 10^{-3}$ m^3 s^{-1}. All polarization curves obtained were characterized by sufficiently long plateaus, which testified to a proper preparation and activation of the surfaces of the cathodes.

RESULTS OF MEASUREMENTS, EXAMPLE OF CALCULATIONS, AND DISCUSSION

According to the pecularities of the electrolytical measurement of the mass transfer coefficients, the heat transfer coefficients resulting from the use of a mass–heat transfer analogy may be valid in the case of a

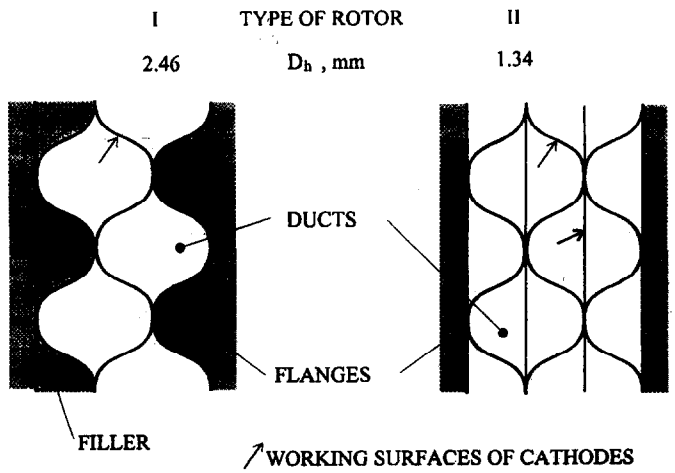

Fig. 1. Sketch of cross-section of test sections at the cylinder surface of the diameter equal to the outside diameter of the rotor.

constant-temperature boundary condition. The calculation of the j_M-factor follows from the information in the Nomenclature: at the same time, values of the needed properties of the electrolyte—at 25°C—are given and discussed in detail in ref. [1].

The experimental results for the type II model—for both horizontal and vertical positions of the axis—are almost identical in the case of individual work of flat and corrugated cathodes, and also in the case of simultaneous work of both of them. This can be observed in Fig. 2. Results for this model were thereinafter calculated as the mean values for the three above-mentioned cathode surfaces, and are shown in Fig. 3(a). Previous results of the author are also presented for comparison. Next, the mean results are presented, in Fig. 3(b), for one of the corrugated surfaces—shown in Fig. 1—of the type I model.

Discrepancies in the results for both horizontal and vertical positions of the axis are as shown in Fig. 4. Absolute values of the discrepancies are in the range of the measurement error. Positive values of the discrepancies are found in the case of the type II model and negative values for the type I model—which differ only in the cross-sections of the ducts and the hydraulic diameter—suggest the independence of the results of the direction of the model axis. That is why the final results were prepared—for both model types—as arithmetic means from values for horizontal

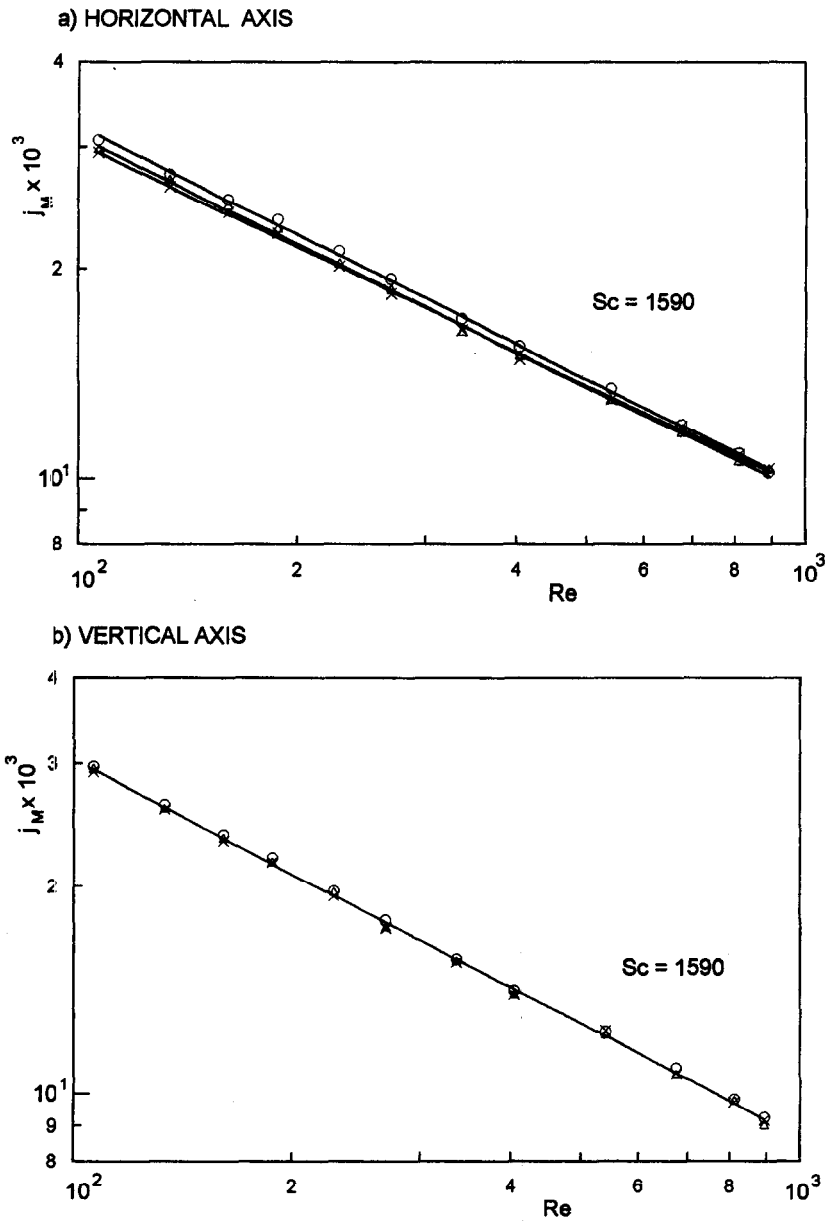

Fig. 2. Results of measurements for particular cathodes of the type II model: (○) flat, (×) corrugated, (Δ) flat and corrugated.

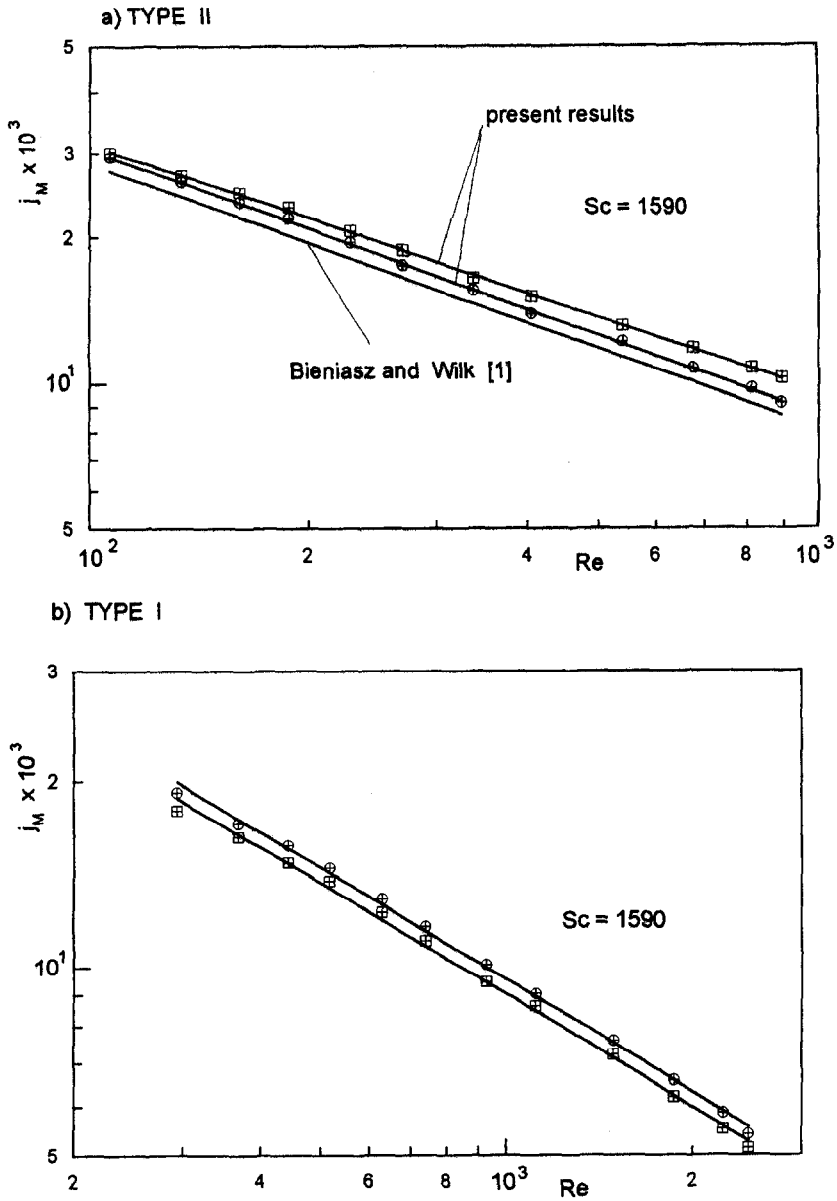

Fig. 3. Mean values—from three independent measurements—of the j_M-factor measured for particular positions of the axes of the models: (⊕) vertical axes, (⊞) horizontal axes.

and vertical cases, which are depicted in Fig. 5 together with the respective correlations.

The correlation for the type II model differs only slightly in the value of the exponent of *Re*, in comparison with that given in ref. [1]: that results in discrepancies smaller than the correlation error. The presented results are, namely, greater than previous ones—once more see Fig. 3(a)—by about 8% at $Re = 110$, and by 11% at $Re = 910$.

Attention should be concentrated on the present result for the type I model, which considerably differs from that in ref. [1], which arose—among other things—from an application of the filler—as shown in Fig. 1—to remove the influence of the presence of side half-ducts on the results of measurements. Thanks to that, the hydraulic diameter, taken from calculations, was precisely equal to that in reality. A great convergence of correlations for both types of model is visible for a common range of *Re*, as depicted in Fig. 6, which presents results for the mean *Sh*.

The results of measurements were used for simple comparative heat transfer coefficient calculations for the type I and II rotors of the same length (50 mm) in an example of dry air at a pressure of 1 bar and a mean temperature of 30°C ($Pr = 0.7$). Other main data are given in Table 3 in ref. [1]. The calculations were based on the j_M vs *Re* correlations—presented in Fig. 5—and on the Chilton–Colburn analogy between

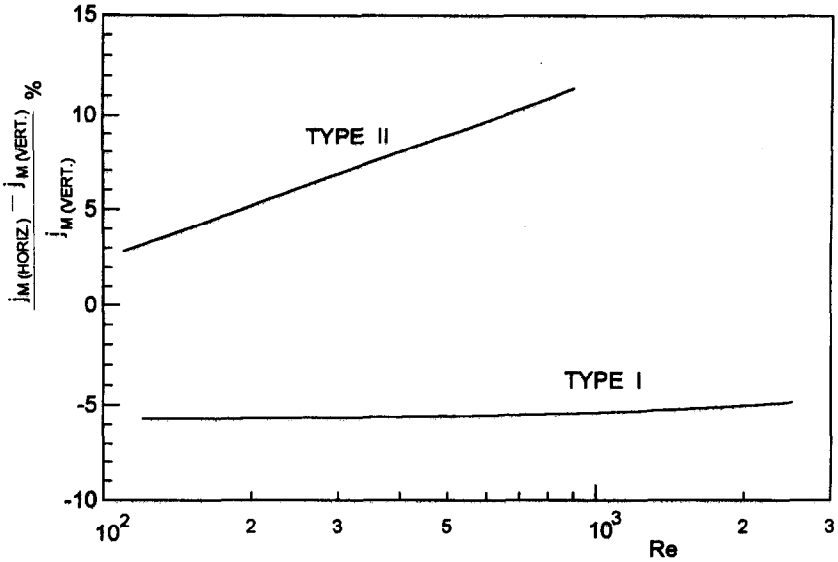

Fig. 4. Relative discrepancies of results obtained at horizontal and vertical axes for both types of model.

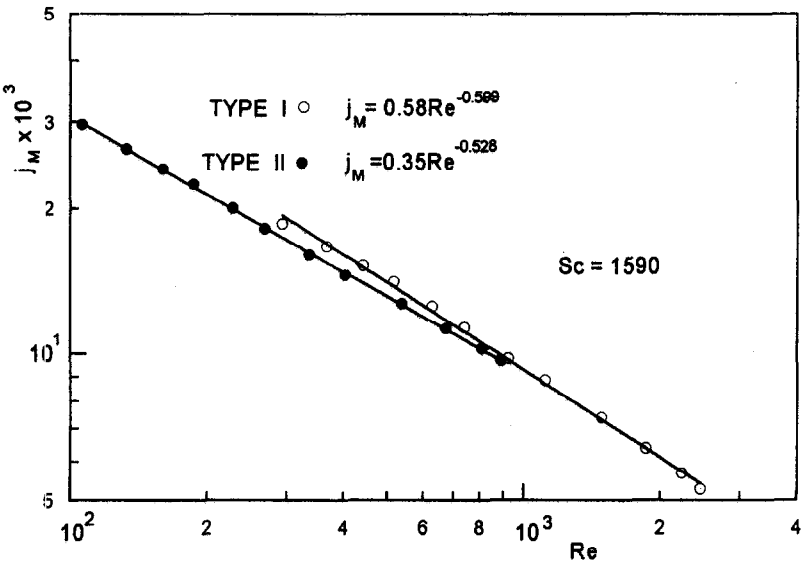

Fig. 5. Mass transfer Chilton–Colburn factor as the arithmetic mean based on values for both horizontal and vertical cases.

mass and heat transfer:

$$j_H = j_M = St_H\, Pr^{2/3}. \quad (1)$$

The effect is that

$$h = 0.58 c_{pg} \rho_g w_g Pr^{-2/3}\, Re^{-0.60} \quad (2)$$

for the type I duct and

$$h = 0.35 c_{pg} \rho_g w_g Pr^{-2/3}\, Re^{-0.53} \quad (3)$$

for the type II duct. The mean values of the heat transfer coefficient are shown in Fig. 7. Next, a comparison of the results for both porous structures was made with regard to two characteristic variants—(a) equal air flux, and (b) equal *Re*—which is presented in Fig. 8. The superiority of the type II pattern over the type I pattern appears in both cases, with regard to the intensity of the heat transfer and the thermal power of the regenerators.

Air fluxes and/or *Re* for both types of real rotor for sucking and forcing regenerators depend, however, strongly on flow resistances under peculiar working conditions. Therefore, the eventual decision on the choice of the rotor pattern and the values of the working parameters of the regenerator has to be preceded by an analysis using both presented mass/heat transfer data and flow characteristics, obtained during separate measurements of the selected system. Experimental flow characteristics for the same types of

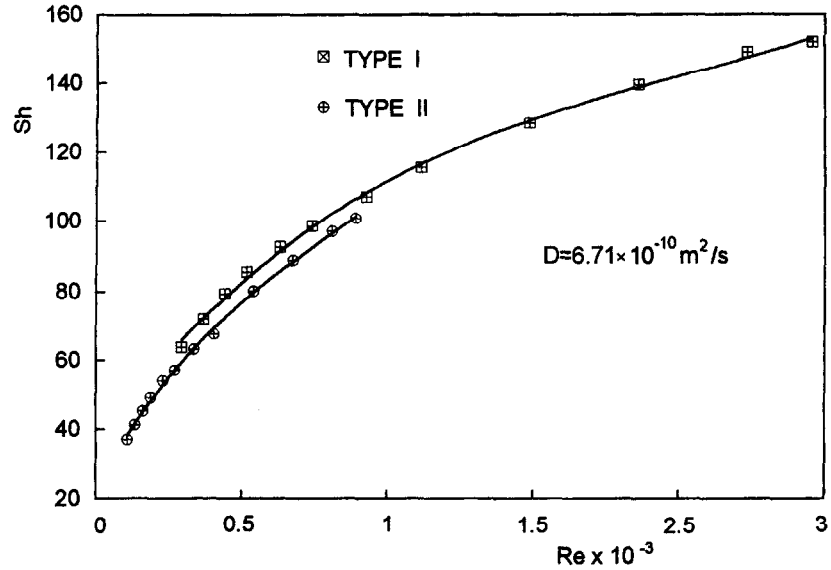

Fig. 6. Sherwood number as the arithmetic mean based on values for both horizontal and vertical cases.

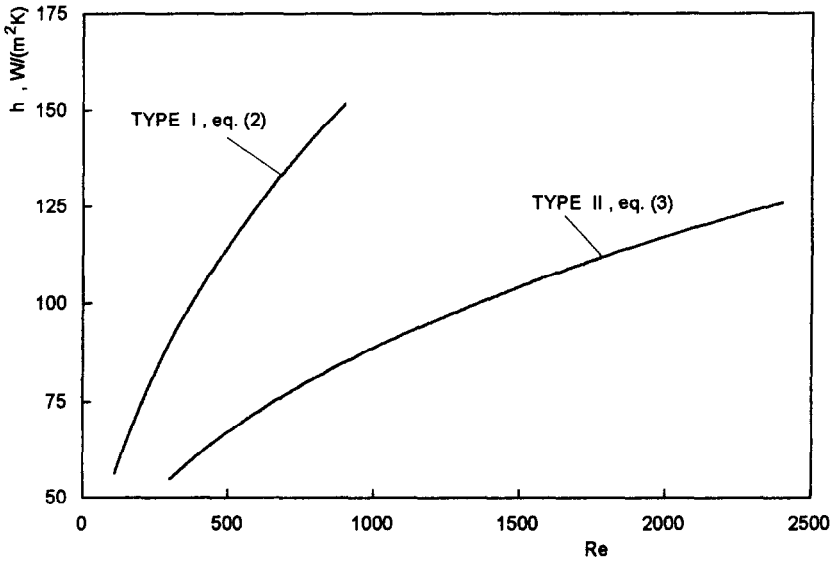

Fig. 7. Heat transfer coefficient in the example specified in the text.

rotors and dimensions as in this work are found in Wawszczak [2, Figs. 11–13] in a form of flux and *Re* vs rotational speed correlations.

The lack of results from the other authors concerning this case does not allow a comparison of the data to be made. Nevertheless, it is worth presenting the results of example calculations for the ducts under consideration, together with the known Lévêque correlation of the mean *Nu*, for the whole surface of the duct, vs the *Gz*, valid for laminar flow in short straight ducts, thus also taking into account the entry effects. This is shown in Fig. 9. The working correlations obtained in a way similar to the case of Fig. 7 are

$$Nu = 0.58\left(\frac{4}{\pi}\frac{L}{D_h}\right)^{0.40} Pr^{-1/15}\, Gz_L^{0.40} \tag{4}$$

for the type I duct and

$$Nu = 0.35\left(\frac{4}{\pi}\frac{L}{D_h}\right)^{0.47} Pr^{-0.14}\, Gz_L^{0.47} \tag{5}$$

for the type II duct. One should remember, looking at Fig. 9, that there is no geometry and flow similarity between this and the Lévêque case.

Secondary flows due to the curvature of the duct axis and the transversal component of the inflow

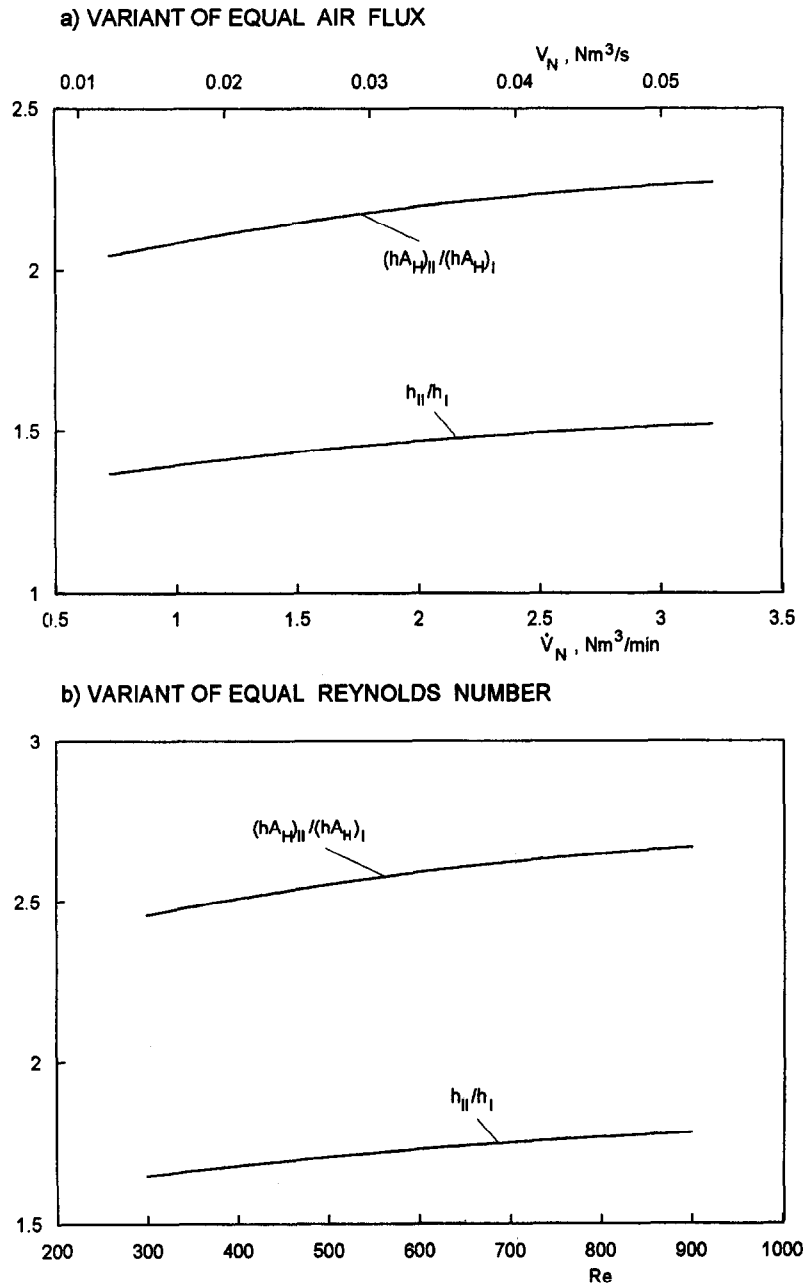

Fig. 8. Comparison of examplary results for both rotor patterns.

stream—entering the duct through, specifically, long triangular side-slots [1]—occur at *Re* for which laminar flow in short straight ordinary ducts exists. They cause the mass/heat transfer to be more intensive, which seems to explain the increase in *Nu* with Gz_L over the values obtained on the basis of Lévêque's equation for both types of duct. Vice versa, for decreasing *Re*—and thereby Gz_L—the influence of the axis curvature and side flows on the fluid flow structure decreases, causing the results of the example calculations to approach those obtained from Lévêque's equation, as shown in Fig. 9.

The uncertainties for all quantities used in the calculations were the same as in ref. [1]—e.g. the accuracy of *Sc* was equal to $\pm 7\%$—with the exception of C_b, for which $\pm 3.5\%$ was obtained. The resulting mean square error for j_M was equal to about $\pm 8.7\%$, for *Re* it was $\pm 7.4\%$, and the error in the j_M vs *Re* correlation was $\pm 17\%$. The above information on the accuracy of mass transfer results is rather precise.

Using the mass transfer results for convective heat transfer calculations, one touches on the difficult problem of additional uncertainties: firstly, of mass transfer modelling of the heat transfer process, and, secondly, of the mass–heat transfer analogy used. In the case of the electrolytic technique, there is no doubt

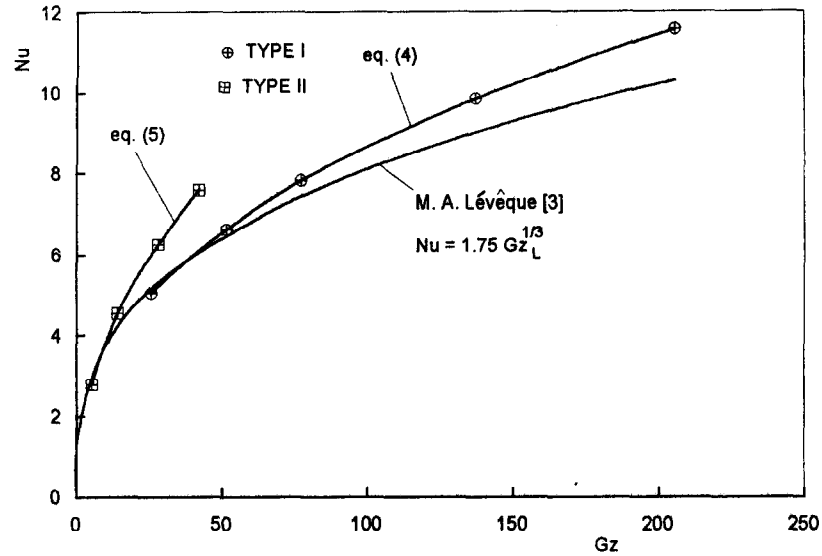

Fig. 9. Results of example in the light of Lévêque's equation.

about the impossibility of fulfilling all the requirements of the phenomenon similarity. In particular, one cannot obtain a similarity of the temperature distribution—the temperature of the electrolyte is constant—and of the material properties for fluids. The last problem especially concerns the *Sc* of working ions in the electrolyte, and the *Pr* of the heat-transferring fluid. The mass–heat transfer analogies assume the equality of both numbers, which cannot be achieved as a rule. That is the case in the example calculations presented in this paper. Secondly, under the same conditions, the results of the heat transfer calculations with the use of mass transfer data and the mass–heat transfer analogy depend on the form of analogy used.

One cannot state exactly the magnitudes of the modelling uncertainties as well as the mass–heat transfer analogy in the case of a new problem. The uncertainties can be assessed only by comparing the results of analogy calculations carried out on the basis of mass transfer experimental data for well-elaborated heat transfer cases. On the basis of their own experience with the electrolytical technique combined with the use of the Chilton–Colburn analogy for calculating the heat transfer data, the authors share the opinion of other researchers that the overall error in *Nu* is comparable with the error in *Nu* obtained as a result of corresponding heat transfer experiments.

CONCLUSIONS

(1) It has been observed that, for horizontal and vertical axes, the position of two different models of the rotor of the sucking and forcing regenerator does not influence the intensity of the convective mass/heat transfer.

(2) The filling of side half-ducts used in a previous model of the type I rotor enabled a better consistency of the real and measured values of D_h to be determined.

(3) By employing a very thin Teflon layer as an insulation between non-acting element surfaces of the model, the flow similarity, and, thereby, accuracy of the results have been improved.

(4) A great convergence of the results for the type II model with the previous ones obtained by the author has been stated, as can be seen in Fig. 3(a).

(5) The results may be used for designing sucking and forcing regenerators, together with the flow characteristic of a peculiar system, owing to the influence of the flow resistance on Reynolds number in the ducts of the rotor at given rotational speeds.

(6) The results of heat transfer calculations for a simple example do not contradict Lévêque's equation, which are valid for laminar flow in short straight ducts.

REFERENCES

1. Bieniasz, B. and Wilk, J., Forced convection mass/heat transfer coefficient at the surface of the rotor of the sucking and forcing regenerative exchanger. *International Journal of Heat and Mass Transfer*, 1995, **38**, 1823–1830.
2. Wawszczak, W., Experimental investigation of a modern high rotating heat exchanger. *Proceedings of the* 1994 *Engineering Systems Design and Analysis Conference, London*, Vol. 8, Part C, 1994, pp. 679–686.
3. Lévêque, M. A., Les lois de la transmission de la chaleur par convection. *Annales des Mines*, 1928, **13**, 201–299, 305–362, 381–415.